British Journal of Mathematics & Computer Science
17(4): 1-19, 2016, Article no.BJMCS.26871
ISSN: 2231-0851

SCIENCEDOMAIN *international*
www.sciencedomain.org

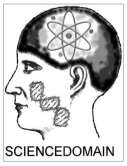

Suppression of Vibrations of a Forced and Self-excited Nonlinear Beam by Using Positive Position Feedback Controller PPF

H. M. Abdelhafez[1*] and M. E. Nassar[1]

[1]Department of Physics and Engineering Mathematics, Faculty of Electronic Engineering, Menoufia University, Menouf 32952, Egypt.

Authors' contributions

This work was carried out in collaboration between both authors. Author HMA designed the study, wrote the protocol and supervised the work. Authors HMA and MEN carried out all laboratories work and performed the statistical analysis. Author HMA managed the analyses of the study. Author MEN wrote the first draft of the manuscript. Author HMA managed the literature searches and edited the manuscript. Both authors read and approved the final manuscript.

Article Information

DOI: 10.9734/BJMCS/2016/26871
Editor(s):
(1) Carlo Bianca, Laboratoire de Physique Théorique de la Matière Condensée, Sorbonne Universités, France.
Reviewers:
(1) Nana Nbendjo, University of Yaoundé I, Cameroon.
(2) Usman A. Marte, University of Maiduguri, Nigeria.
(3) Changzhao Qian, Xiamen University of Technology, China.
Complete Peer review History: http://sciencedomain.org/review-history/15199

Original Research Article

Received: 7th May 2016
Accepted: 14th June 2016
Published: 28th June 2016

Abstract

This paper presents a quantitative analysis on the nonlinear behavior of a forced and self-excited beam coupled with a positive position feedback controller PPF. Such that the external excitation is a harmonic motion on the support of the cantilever beam. Self-excitation is caused by fluid flow and modelled by a nonlinear damping with a negative linear part (Rayleigh's function). Self-excitation can build up oscillations even in the absence of external forces. Also self-excitation can interact with the external excitation and lead system to vibrate with a quasi-periodic motion and to be unstable. This problem is treated here by using PPF controller. It is assumed that the beam vibrates in the presence of external harmonic excitation close to its natural frequency and one to one internal resonance. Multiple scales perturbation technique MSPT is used to get a first order approximate solution of this system. The stability of the steady state solution is investigated by using the frequency-response equations. The effects of different controller parameters on beam vibrations are studied and optimum conditions for system operation are deduced. Finally, all analytical results are validated by using numerical solution.

**Corresponding author: E-mail: hassanma0@yahoo.com;*

Keywords: *Active control; multiple scales method; nonlinear beam oscillations; positive position feedback controller; self-excited vibrations.*

NOMENCLATURES

$x_1, \dot{x}_1, \ddot{x}_1$	:	*Displacement, velocity and acceleration of the beam, respectively.*
$x_2, \dot{x}_2, \ddot{x}_2$	:	*Displacement, velocity and acceleration of the controller, respectively.*
α_1	:	*Negative viscous damping coefficient of the beam.*
β_1	:	*The cubic damping coefficient of the beam.*
ω_1	:	*Ratio of the natural frequency of the composite beam with the lumped mass with respect to that of the reference beam without the lumped mass.*
γ_1	:	*Coefficient describes the beam geometrical nonlinearity.*
δ	:	*Coefficient describes the beam inertia nonlinearity.*
x_0	:	*Amplitude of the support motion.*
Ω	:	*Frequency of the support motion.*
μ	:	*Constant.*
λ_1	:	*The control signal gain.*
α_2	:	*Linear damping coefficient of the controller.*
ω_2	:	*Controller natural frequency.*
γ_2	:	*Cubic nonlinearity coefficient of the controller.*
λ_2	:	*Positive control feedback gain.*

1 Introduction

In mechanics, self-excited oscillations come from nonlinearity of the exciting force through absorption of energy from a continuous flow of energy. Dry friction and fluid flow are well-known sources of self-excited oscillations. An oscillations can be built up even in the absence of external forces due to self-excitations.

The quenching phenomenon of self-excited systems was extensively studied by Abadi [1]. El-Badawy and Nasr El-Deen [2] applied a nonlinear controller based on saturation phenomenon to suppress vibrations of a self-excited system modeled by the van der Pol oscillator. Analytical solutions illustrated good vibration suppression when system is perfectly tuned i.e. the frequency of the controller was half of the fundamental plant's frequency. Jun et al. [3] applied a nonlinear saturation controller NSC with van der Pol oscillator and additionally investigated the influence of feedback gains by using perturbation and direct numerical integration solutions. In [4], the behavior of a micro beam is improved by using a nonlinear feedback controller. Also authors presented a novel control design that regulates the pass band of the considered micro beam. Golnaraghi [5] proposed a passive vibration controller for a cantilever beam by using a sliding mass-spring-dashpot mechanism placed at the free end of a cantilever. Duquette [6,7] presented a similar approach which uses a DC motor with a pendulum attached to the motor shaft to play the controller's role. Their results showed that this controller is most effective in controlling large amplitude and low frequency oscillations which are typical for large flexible structures. A saturation controller which uses standard (piezoelectric) PZT patches was applied to a nonlinear system in [8]. Authors deduced that NSC is globally stable. Pai et al. [9] used a NSC to suppress steady state vibrations of a cantilever beam with quadratic nonlinearities in presence of 2:1 internal resonances. Also authors used PZT patches as actuators and sensors. Systems with self and parametric or external excitations were intensively studied in [10-12]. Authors found that interactions between self and periodically excited systems lead to a quasi-periodic response, but in selected frequency domains the frequency quenching phenomenon is seen to take place. Abadi [1] and Verhulst [13] studied extensively the quenching phenomenon of self-excited systems which

have an important practical meanings in fluid-structure interactions. Szabelski and Warminski [14–16] studied a self-exited system under parametric and external excitation sources. They found that the frequency locking zones may change radically for some combinations of parameters, small external force may change the system's response and internal loop occurs in the amplitude-frequency response curve. Moreover, interactions between self and parametric or external excitations may lead to chaotic or hyper chaotic dynamics as shown in [17,18]. In [19] authors applied NSC for a forced and self-excited strongly nonlinear beam structure to reduce self and externally excited vibrations. They found that the system might lose stability when the two type excitations interact near the fundamental resonance zone. Jian Xu and his co-authors in [20] improved a nonlinear saturation controller and utilized it to reduce high-amplitude vibrations of a flexible, geometrically nonlinear beam-like structure.

In this work, Positive position feedback PPF controller is applied to reduce the vibrations of a forced and self-excited nonlinear beam. Systems with self-excitation are common in applications of solid or fluid mechanics [1]. Self-excitation can build up oscillations even in the absence of external forces. Also self-excitation can interact with the external excitation and lead system to vibrate with a quasi-periodic motion and to be unstable. External excitation is a harmonic excitation on the support of the cantilever beam. Self-excitation is caused by fluid flow and modelled by a nonlinear damping with a negative linear part. MSPT is applied to obtain a first-order approximate solution in the simultaneous resonance case. The equilibrium solution curves are plotted for various values of controller parameters. The stability of the steady state solution is investigated by using frequency-response equations. The approximate analytical solution is verified numerically.

2 Model of the Structure

The model of the beam is presented in Fig. 1 as given in [19]. Where *M* is a lumped mass attached at the end of the beam, *L*, *h* are the length and the height of the beam respectively, and b is the width of the beam.

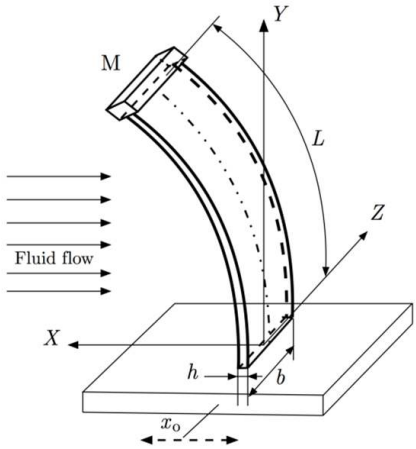

Fig. 1. Model of the nonlinear beam with self and external excitations

The cantilever beam is mounted on an armature of an electro dynamic shaker which is a source of excitation along the *X* axis. In practice, for example, this model can be used to describe the wing of a plane such that, the wing of plane is suspended to external excitation from plane body and self-excitation from the wind flow. The external excitation is written as,

$$x = x_0 \sin(\Omega t). \tag{1}$$

The differential equation of the beam (the plant) is given in [19] in the dimensionless form as follows:

$$\ddot{x}_1 + (-\alpha_1 \dot{x}_1 + \beta_1 \dot{x}_1^3) + \omega_1^2 x_1 + \gamma_1 x_1^3 + \delta(x_1 \dot{x}_1^2 + x_1^2 \ddot{x}_1) = \mathrm{x}_0 \mu \Omega^2 \sin(\Omega \mathrm{t}) + U. \tag{2}$$

Self-excitation is represented by a nonlinear damping with a negative linear part (Rayleigh's function). A control force *U* is added to right hand side of differential equation (2). In this work positive position feedback controller (PPF) is investigated so the control force *U* is given by

$$U = \lambda_1 x_2. \tag{3}$$

The equation which governs the dynamics of this controller (PPF) is suggested as,

$$\ddot{x}_2 + \alpha_2 \dot{x}_2 + \omega_2^2 x_2 + \gamma_2 x_2^3 = \lambda_2 f_f(\mathrm{t}). \tag{4}$$

Where $f_f(t) = x_1$ is the feedback signal from the beam. So the closed loop system equations are:

$$\ddot{x}_1 + (-\alpha_1 \dot{x}_1 + \beta_1 \dot{x}_1^3) + \omega_1^2 x_1 + \gamma_1 x_1^3 + \delta(x_1 \dot{x}_1^2 + x_1^2 \ddot{x}_1) = x_0 \mu \Omega^2 \sin(\Omega t) + \lambda_1 x_2, \tag{5}$$

$$\ddot{x}_2 + \alpha_2 \dot{x}_2 + \omega_2^2 x_2 + \gamma_2 x_2^3 = \lambda_2 x_1. \tag{6}$$

3 Perturbation Analysis

Using multiple scales perturbation technique (MSPT) [21]. Assume that the system is weakly nonlinear. We can obtain a first-order approximate solution of equations (5) and (6) by seeking the solution in the forms

$$x_1(T_0, T_1, \varepsilon) = x_{10}(T_0, T_1) + \varepsilon x_{11}(T_0, T_1), \tag{7}$$

$$x_2(T_0, T_1, \varepsilon) = x_{20}(T_0, T_1) + \varepsilon x_{21}(T_0, T_1). \tag{8}$$

Such that ε is small dimensionless parameter $\varepsilon << 1$, $T_0 = t$, $T_1 = \varepsilon t$ are fast and slow time scales respectively. Time derivatives in terms of T_0, T_1 are:

$$\frac{d}{dt} = D_0 + \varepsilon D_1, \frac{d^2}{dt^2} = D_0^2 + 2\varepsilon D_0 D_1, D_j = \frac{\partial}{\partial T_j}, j = 0,1. \tag{9}$$

To obtain a uniformly valid approximate solution of this problem, we order the dimensionless parameters of the system by the formal small parameter ε as follows:

$$\alpha_1 = \varepsilon \hat{\alpha}_1, \beta_1 = \varepsilon \hat{\beta}_1, \gamma_1 = \varepsilon \hat{\gamma}_1, \delta = \varepsilon \hat{\delta}, \mu = \varepsilon \hat{\mu}, \lambda_1 = \varepsilon \hat{\lambda}_1, \alpha_2 = \varepsilon \hat{\alpha}_2, \gamma_2 = \varepsilon \hat{\gamma}_2, \lambda_2 = \varepsilon \hat{\lambda}_2. \tag{10}$$

Substitute equations (7-10) into (5) and (6) and equate coefficients of like powers of ε. So we can obtain the following set of ordinary differential equations

$$(D_0^2 + \omega_1^2) x_{10} = 0, \tag{11}$$

$$(D_0^2 + \omega_2^2) x_{20} = 0, \tag{12}$$

$$(D_0^2+\omega_1^2)x_{11} = x_0\,\hat{\mu}\,\Omega^2\sin(\Omega\,T_0) - \hat{\gamma}\,x_{10}^3 + \hat{\lambda}_1\,x_{20} + \hat{\alpha}_1\,D_0\,x_{10} - \hat{\delta}\,x_{10}\,(D_0\,x_{10})^2 - \hat{\beta}_1(D_0\,x_{10})^3 - 2D_0D_1\,x_{10} - \hat{\delta}\,x_{10}^2D_0^2\,x_{10}, \tag{13}$$

$$(D_0^2+\omega_2^2)x_{21} = \hat{\lambda}_2\,x_{10} - \hat{\gamma}_2\,x_{20}^3 - \hat{\alpha}_2\,D_0\,x_{20} - 2D_0D_1x_{20}. \tag{14}$$

The general solution of (11) and (12) can be expressed in the forms

$$x_{10}(T_0,T_1) = A(T_1)\,e^{i\omega_1 T_0} + \overline{A}(T_1)\,e^{-i\omega_1 T_0}, \tag{15}$$

$$x_{20}(T_0,T_1) = B(T_1)\,e^{i\omega_2 T_0} + \overline{B}(T_1)\,e^{-i\omega_2 T_0}. \tag{16}$$

The coefficients $A(T_1)$, $B(T_1)$ are unknown functions of T_1. They can be determined later by eliminating the secular and small devisor terms. By Substituting (15), (16) in to (13), (14) we can get,

$$(D_0^2+\omega_1^2)\,x_{11} = (i\,\hat{\alpha}_1\,\omega_1\,A + 2\,\hat{\delta}\,\omega_1^2A^2\overline{A} - 3\,i\,\hat{\beta}_1\,\omega_1^3A^2\overline{A} - 3\,\hat{\gamma}_1A^2\overline{A} - 2\,i\,\omega_1\,D_1A)e^{i\omega_1 T_0} + (2\hat{\delta}\,\omega_1^2\,A^3 + i\,\hat{\beta}_1\,\omega_1^3\,A^3 - \hat{\gamma}_1\,A^3)e^{3i\omega_1T_0} + \hat{\lambda}_1\,B\,e^{i\omega_2 T_0} - \frac{1}{2}\,i\,x_0\,\hat{\mu}\;\Omega^2\,e^{i\Omega T_0} + cc, \tag{17}$$

$$(D_0^2+\omega_2^2)x_{21} = (-i\,B\,\omega_2\,\hat{\alpha}_2 - 3\,\hat{\gamma}_2\,B^2\overline{B} - 2i\,\omega_2D_1B)e^{i\omega_2 T_0} - \hat{\gamma}_2\,B^3e^{3i\omega_2 T_0} + \hat{\lambda}_2\,A\,e^{i\omega_1 T_0} + cc. \tag{18}$$

Where cc stands for the complex conjugate of the preceding terms and the over bar denotes the complex conjugate functions. The particular solution of (17) and (18) are:

$$x_{11} = \frac{-1}{8\,\omega_1^2}(2\hat{\delta}\,\omega_1^2\,A^3 + i\,\hat{\beta}_1\,\omega_1^3\,A^3 - \hat{\gamma}_1\,A^3)e^{3i\omega_1T_0} + \frac{\hat{\lambda}_1\,B}{(\omega_1^2-\omega_2^2)}e^{i\omega_2 T_0} - \frac{i\,x_0\,\hat{\mu}\;\Omega^2}{2(\omega_1^2-\Omega^2)}e^{i\Omega T_0} + cc, \tag{19}$$

$$x_{21} = \frac{\hat{\gamma}_2\,B^3}{8\,\omega_2^2}e^{3i\omega_2 T_0} + \frac{\hat{\lambda}_2\,A}{(\omega_2^2-\omega_1^2)}e^{i\omega_1 T_0} + cc. \tag{20}$$

From (19), (20) we can deduce that the resonance conditions in this approximation order are:

(I) Primary resonance: $\Omega = \omega_1$,

(ii) Internal resonance: $\omega_2 = \omega_1$,

(iii) Simultaneous resonance: $\Omega = \omega_1$ and $\omega_2 = \omega_1$.

In this paper we study the case of simultaneous resonance ($\Omega = \omega_1$ and $\omega_2 = \omega_1$). Closeness of simultaneous resonance can be described by using detuning parameters σ_1 and σ_2 as follows

$$\Omega = \omega_1 + \sigma_1 = \omega_1 + \varepsilon\hat{\sigma}_1,\ \omega_2 = \omega_1 + \sigma_2 = \omega_1 + \varepsilon\hat{\sigma}_2. \tag{21}$$

By inserting (21) into the secular and small devisor terms in (17) and (18), one finds the solvability conditions

$$\begin{aligned}(i\,A\,\omega_1\,\hat{\alpha}_1 + 2\,\hat{\delta}\,\omega_1^2\,A^2\overline{A} - 3\,i\,\hat{\beta}_1\,\omega_1^3\,A^2\overline{A} - 3\,\hat{\gamma}_1\,A^2\overline{A} - 2i\omega_1\,D_1A)\,e^{i\,\omega_1 T_0}\\ -\frac{1}{2}\,i\,x_0\,\hat{\mu}\;\Omega^2\,e^{iT_0(\omega_1+\varepsilon\hat{\sigma}_1)} + \hat{\lambda}_1 B\,e^{iT_0(\omega_1+\varepsilon\hat{\sigma}_2)} = 0,\end{aligned} \tag{22}$$

$$\left(-i\,\hat{\alpha}_2\,\omega_2\,B - 3\,\hat{\gamma}_2\,B^2\overline{B} - 2\,i\,\omega_2\,D_1B\right)e^{i\,\omega_2 T_0} + \hat{\lambda}_2\,A\,e^{iT_0(\omega_2-\varepsilon\hat{\sigma}_2)} = 0. \tag{23}$$

By dividing (22) and (23) by $e^{i\,\omega_1 T_0}$ and $e^{i\,\omega_2 T_0}$ respectively, we can get

$$\begin{aligned}i\,A\,\omega_1\,\hat{\alpha}_1 + 2\,\hat{\delta}\,\omega_1^2\,A^2\overline{A} - 3\,i\,\hat{\beta}_1\,\omega_1^3\,A^2\overline{A} - 3\,\hat{\gamma}_1\,A^2\overline{A} - 2i\omega_1\,D_1A\\ -\frac{1}{2}\,i\,x_0\,\hat{\mu}\;\Omega^2\,e^{i\varepsilon\hat{\sigma}_1 T_0} + \hat{\lambda}_1 B\,e^{i\varepsilon\hat{\sigma}_2 T_0} = 0,\end{aligned} \tag{24}$$

$$i\,\hat{\alpha}_2\,\omega_2\,B + 3\,\hat{\gamma}_2\,B^2\overline{B} + 2\,i\,\omega_2\,D_1B - \hat{\lambda}_2\,A\,e^{-i\,\varepsilon\hat{\sigma}_2 T_0} = 0. \tag{25}$$

To analyze the solution of (24) and (25), express A and B in polar form as follows

$$A = \frac{a_1}{2}e^{i\beta_1},\ D_1A = \frac{a_1'}{2}e^{i\beta_1} + i\frac{a_1\beta_1'}{2}e^{i\beta_1}, \tag{26}$$

$$B = \frac{a_2}{2}e^{i\beta_2},\ D_1B = \frac{a_2'}{2}e^{i\beta_2} + i\frac{a_2\beta_2'}{2}e^{i\beta_2}. \tag{27}$$

Where prime denotes derivative w.r.t. T_1, a_1 and a_2 are the steady-state displacement amplitudes of the beam and controller, respectively and β_1, β_2 are the phases of the motion. By inserting (26) and (27) into (24) and (25) and returning each scaled parameter back to its real value we can get

$$\dot{a}_1 = \frac{-4\,\mu\,x_0\,\Omega^2\cos(\varphi_1) + 4\,\alpha_1\,\omega_1\,a_1 - 3\,\beta_1\,\omega_1^3\,a_1^3 + 4\,\lambda_1\,a_2\sin(\varphi_2)}{8\,\omega_1}, \tag{28}$$

$$\dot{\beta}_1 = \frac{-4\,\mu\,x_0\,\Omega^2\sin(\varphi_1) - 2\delta\,\omega_1^2\,a_1^3 + 3\,\gamma_1\,a_1^3 - 4\,\lambda_1\,a_2\cos(\varphi_2)}{8\,\omega_1\,a_1}, \tag{29}$$

$$\dot{a}_2 = \frac{-\lambda_2\,a_1\sin(\varphi_2) - \alpha_2\,\omega_2\,a_2}{2\,\omega_2}, \tag{30}$$

$$\dot{\beta}_2 = \frac{3\,\gamma_2\,a_2^3 - 4\,\lambda_2\,a_1\cos(\varphi_2)}{8\,\omega_2\,a_2}. \tag{31}$$

Where dot represents derivative w.r.t. t and

$$\varphi_1 = \varepsilon\,\hat{\sigma}_1\,T_0 - \beta_1 = \sigma_1\,t - \beta_1, \quad \varphi_2 = \varepsilon\,\hat{\sigma}_2\,T_0 - \beta_1 + \beta_2 = \sigma_2\,t - \beta_1 + \beta_2. \tag{32}$$

To eliminate $\dot{\beta}_1$ and $\dot{\beta}_2$ from equations (29) and (31), differentiate (32) w.r.t. t. So we can get

$$\dot{\beta}_1 = \sigma_1 - \dot{\varphi}_1,\ \dot{\beta}_2 = (\dot{\varphi}_2 - \dot{\varphi}_1 + \sigma_1 - \sigma_2). \tag{33}$$

By inserting (33) in to (29) and (31) respectively, we can get

$$\dot{\varphi}_1 = \frac{4\,\mu\,x_0\,\Omega^2\sin(\varphi_1) + 8\,\sigma_1\,\omega_1\,a_1 + 2\,\delta\,\omega_1^2\,a_1^3 - 3\,\gamma_1\,a_1^3 + 4\,\lambda_1\,a_2\cos(\varphi_2)}{8\,\omega_1\,a_1}, \tag{34}$$

$$\begin{aligned}\dot{\varphi}_2 = \frac{1}{8\,\omega_1\,\omega_2\,a_1\,a_2}\Big(&-4\,\lambda_2\,\omega_1\,a_1^2\cos(\varphi_2) + 4\,\mu\,x_0\,\omega_2\,\Omega^2\,a_2\sin(\varphi_1) + 8\,\omega_1\,\omega_2\,\sigma_2\,a_1\,a_2 \\ &+ 2\,\delta\,\omega_1^2\,\omega_2\,a_1^3\,a_2 - 3\,\gamma_1\,\omega_2\,a_1^3\,a_2 + 4\,\lambda_1\,\omega_2\,a_2^2\cos(\varphi_2) + 3\,\gamma_2\,\omega_1\,a_1\,a_2^3\Big).\end{aligned} \tag{35}$$

The autonomous Amplitude-phase modulating equations can be obtained from (28), (30), (34) and (35) as follows

$$\left.\begin{aligned}\dot{a}_1 &= \frac{-4\,\mu\,x_0\,\Omega^2\cos(\varphi_1) + 4\,\alpha_1\,\omega_1\,a_1 - 3\,\beta_1\,\omega_1^3\,a_1^3 + 4\,\lambda_1\,a_2\sin(\varphi_2)}{8\,\omega_1}, \\ \dot{\varphi}_1 &= \frac{4\,\mu\,x_0\,\Omega^2\sin(\varphi_1) + 8\,\sigma_1\,\omega_1\,a_1 + 2\,\delta\,\omega_1^2\,a_1^3 - 3\,\gamma_1\,a_1^3 + 4\,\lambda_1\,a_2\cos(\varphi_2)}{8\,\omega_1\,a_1}, \\ \dot{a}_2 &= \frac{-\lambda_2\,a_1\sin(\varphi_2) - \alpha_2\,\omega_2\,a_2}{2\,\omega_2}, \\ \dot{\varphi}_2 &= \frac{1}{8\,\omega_1\,\omega_2\,a_1\,a_2}\Big(-4\,\lambda_2\,\omega_1\,a_1^2\cos(\varphi_2) + 4\,\mu\,x_0\,\omega_2\,\Omega^2\,a_2\sin(\varphi_1) + 8\,\omega_1\,\omega_2\,\sigma_2\,a_1\,a_2 \\ &\quad + 2\,\delta\,\omega_1^2\,\omega_2\,a_1^3\,a_2 - 3\,\gamma_1\,\omega_2\,a_1^3\,a_2 + 4\,\lambda_1\,\omega_2\,a_2^2\cos(\varphi_2) + 3\,\gamma_2\,\omega_1\,a_1\,a_2^3\Big).\end{aligned}\right\} \tag{36}$$

4 Equilibrium Solution

To obtain the steady state response of both the beam and the controller we must set the values

$$\dot{a}_1 = \dot{a}_2 = \dot{\varphi}_1 = \dot{\varphi}_2 = 0. \tag{37}$$

By Substituting (37) into (33) we can get

$$\dot{\beta}_1 = \sigma_1,\ \dot{\beta}_2 = \sigma_1 - \sigma_2. \tag{38}$$

By substituting (37) and (38) in to (28) to (31) we can get

$$4\,\alpha_1\,\omega_1\,a_1 - 3\,\beta_1\,\omega_1^3\,a_1^3 - 4\,\mu\,x_0\,\Omega^2\cos(\varphi_1) + 4\,\lambda_1\,a_2\sin(\varphi_2) = 0, \tag{39}$$

$$8\,\sigma_1\,\omega_1\,a_1+2\delta\,\omega_1^2\,a_1^3-3\,\gamma_1\,a_1^3+4\,\mu\,x_0\,\Omega^2\sin(\varphi_1)+4\,\lambda_1\,a_2\cos(\varphi_2)=0, \tag{40}$$

$$\alpha_2\,\omega_2\,a_2+\lambda_2\,a_1\sin(\varphi_2)=0, \tag{41}$$

$$3\,\gamma_2\,a_2^3-8(\sigma_1-\sigma_2)\,\omega_2\,a_2-4\,\lambda_2\,a_1\cos(\varphi_2)=0. \tag{42}$$

From (41) and (42) we can get values of $\sin(\varphi_2)$ and $\cos(\varphi_2)$ as follows

$$\sin(\varphi_2)=-\frac{\alpha_2\,\omega_2\,a_2}{\lambda_2\,a_1}, \tag{43}$$

$$\cos(\varphi_2)=\frac{a_2\left(-8\,\sigma_1\,\omega_2+8\,\sigma_2\,\omega_2+3\,\gamma_2\,a_2^2\right)}{4\,\lambda_2\,a_1}. \tag{44}$$

By substituting (43) and (44) into (39) and (40) respectively, we can obtain

$$\cos(\varphi_1)=\frac{4\,\alpha_1\,\lambda_2\,\omega_1\,a_1^2-3\,\beta_1\,\lambda_2\,\omega_1^3\,a_1^4-4\,\alpha_2\,\lambda_1\,\omega_2\,a_2^2}{4\mu\,\Omega^2\,x_0\,\lambda_2\,a_1}, \tag{45}$$

$$\begin{aligned}\sin(\varphi_1)=\frac{1}{4\,\mu\,\Omega^2\,x_0\,\lambda_2\,a_1}\Big(&-8\,\lambda_2\,\sigma_1\,\omega_1\,a_1^2+3\,\gamma_1\,\lambda_2\,a_1^4-2\,\delta\,\lambda_2\,\omega_1^2\,a_1^4\\&+8\,\lambda_1\,\sigma_1\,\omega_2\,a_2^2-8\,\lambda_1\,\sigma_2\,\omega_2\,a_2^2-3\,\gamma_2\,\lambda_1\,a_2^4\Big).\end{aligned} \tag{46}$$

By squaring and adding (43) and (44) we can deduce the first closed form equation as follows

$$a_2^2\left(\left(3\,\gamma_2\,a_2^2-8\,\sigma_1\,\omega_2+8\,\sigma_2\,\omega_2\right)^2+16\,\alpha_2^2\,\omega_2^2\right)=16\,\lambda_2^2\,a_1^2, \tag{47}$$

$$\begin{aligned}&\left(-4\alpha_1\lambda_2\omega_1a_1^2+4\alpha_2\lambda_1\omega_2a_2^2+3\beta_1\lambda_2\omega_1^3a_1^4\right)^2\\&+\left(\lambda_2\left(a_1^4\left(2\delta\omega_1^2-3\gamma_1\right)+8\sigma_1\omega_1a_1^2\right)+\lambda_1a_2^2\left(3\gamma_2a_2^2-8\sigma_1\omega_2+8\sigma_2\omega_2\right)\right)^2=16\lambda_2^2\mu^2x_0^2\Omega^4a_1^2.\end{aligned} \tag{48}$$

Equations (47) and (48) are the frequency response equations. They describe the system steady state solutions behavior for the practical case i.e. ($a_1\neq 0,\ a_2\neq 0$).

5 Stability Analysis

Jacobian matrix J of the right-hand side of equations (36) can be used to study the stability of the equilibrium solution. To derive the stability criteria, we need to examine the behavior of small deviations from the equilibrium solutions. Thus we assume that

$$\begin{aligned}&a_1=a_{11}+a_{10},\ a_2=a_{21}+a_{20},\ \varphi_1=\varphi_{11}+\varphi_{10},\ \varphi_2=\varphi_{21}+\varphi_{20}\\&\dot{a}_1=\dot{a}_{11},\ \dot{a}_2=\dot{a}_{21},\ \dot{\varphi}_1=\dot{\varphi}_{11},\ \dot{\varphi}_2=\dot{\varphi}_{21}.\end{aligned} \tag{49}$$

Such that a_{10}, φ_{10}, a_{20}, φ_{20} denotes the equilibrium solution which satisfy closed form equation (47) and (48) and a_{11}, φ_{11}, a_{21}, φ_{21} are perturbations which are assumed to be small compared to a_{10}, φ_{10}, a_{20}, φ_{20}. By substituting (49) into (36) and keeping linear terms in a_{11}, φ_{11}, a_{21}, φ_{21} we can get,

$$\dot{a}_{11} = r_{11}a_{11}+r_{12}\varphi_{11} + r_{13}a_{21} + r_{14}\varphi_{21}, \tag{50}$$

$$\dot{\varphi}_{11} = r_{21}a_{11}+r_{22}\varphi_{11} + r_{23}a_{21} + r_{24}\varphi_{21}, \tag{51}$$

$$\dot{a}_{21} = r_{31}a_{11}+r_{32}\varphi_{11} + r_{33}a_{21} + r_{34}\varphi_{21}, \tag{52}$$

$$\dot{\varphi}_{21} = r_{41}a_{11}+r_{42}\varphi_{11} + r_{43}a_{21} + r_{44}\varphi_{21}. \tag{53}$$

The characteristic determinant of equations (50) to (53) can be expressed as follows,

$$\begin{vmatrix} r_{11}-\lambda & r_{12} & r_{13} & r_{14} \\ r_{21} & r_{22}-\lambda & r_{23} & r_{24} \\ r_{31} & r_{32} & r_{33}-\lambda & r_{34} \\ r_{41} & r_{42} & r_{43} & r_{44}-\lambda \end{vmatrix} = 0 \tag{54}$$

Thus, the stability of the steady-state solution depends on the eigenvalues λ of the Jacobian matrix $[J]$, which can be obtained from (54). Such that r_{ij} where $i = 1,2,3,4$ and $j = 1,2,3,4$ are given in the appendix.

6 Results and Discussion

In this section the steady-state response of the system is discussed extensively. The dimensionless parameters of the system take the values $\alpha_1 = 0.01$, $\beta_1 = 0.05$, $\omega_1 = 3.06309$, $\gamma_1 = 14.4108$, $\delta = 3.2746$, $\mu = 0.89663$. The amplitude and frequency of excitation vary respectively, in these ranges $x_0 \in (0,0.1)$ and $\Omega \in (1.5,4.5)$ approximately. The PPF controller parameters are chosen as $\alpha_2 = 0.05$, $\omega_2 = \omega_1 + \sigma_2$, $\sigma_2 = 0$, $\gamma_2 = 0$ and $\lambda_1 = \lambda_2 = 5$ unless specifying otherwise. In the obtained figures solid lines correspond to stable solutions while dashed lines correspond to unstable.

6.1 Nonlinear composite beam without control

Self-excitation in the uncontrolled system can build up oscillations even in the absence of external forces $x_0 = 10^{-8}$ as shown in Fig. 2. If we compare between Figs. 2(a) and 2(b) we can see that, When Self-excitation increases, the transient region in the resulted oscillations decreases and the steady state displacement amplitude increases.

When there is an external excitation to the system $x_0 = 0.01$ as in Fig. 3. Self-excitation can interact with the external excitation and may lead system to vibrate with a quasi-periodic motion and to be unstable. When the effect of external excitation is greater than the effect self-excitation, the beam vibrates periodically. However, the beam vibrates with a quasi-periodic motion if the effect of self-excitation is greater than the effect of external excitation. It can be seen from Figs. 3(a) and 3(b) that, when self-excitation increases in Fig. 3(b) than that in Fig. 3(a), the beam's motion becomes a quasi-periodic motion.

Fig. 4 presents the frequency response curve (FRC) of the beam without control under different values of amplitude of the support motion x_0. It can be seen that there are unstable regions in the FRC curve which corresponds to a quasi-periodic motion. In these unstable regions, roots of the characteristic equation are conjugate complex numbers with positive real parts. In stable regions the beam vibrates periodically. It can be seen that the steady state displacement amplitude of the beam increases as the Amplitude of the support motion x_0 increases. Also the curve is bent to the left denoting a softening effect and the jump phenomena appear clearly due to the domination of the nonlinearity. We try to treat these problems by using PPF controller.

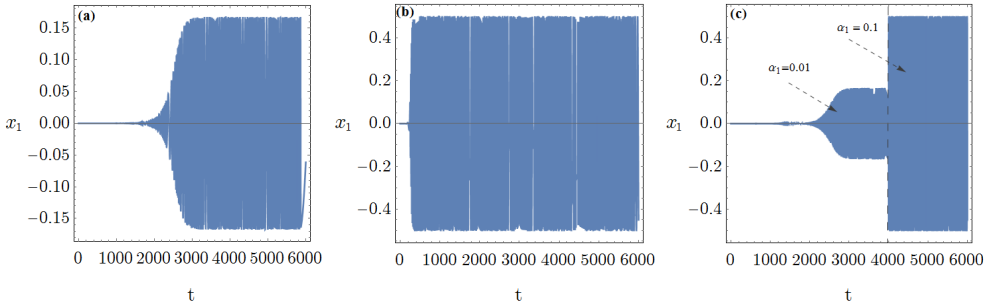

Fig. 2. (a) Time history of the uncontrolled system at $\alpha_1 = 0.01$, (b) Time history of the uncontrolled system at $\alpha_1 = 0.1$ and (c) Comparison between two cases (a) and (b) all at $x_0 = 10^{-8}$

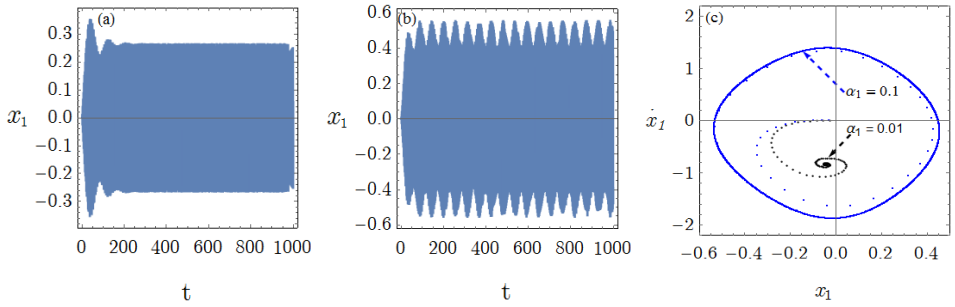

Fig. 3. (a) Time history of the uncontrolled system at $\alpha_1 = 0.01$, (b) Time history of the uncontrolled system at $\alpha_1 = 0.1$ and (c) Poincare map all at $x_0 = 0.01$

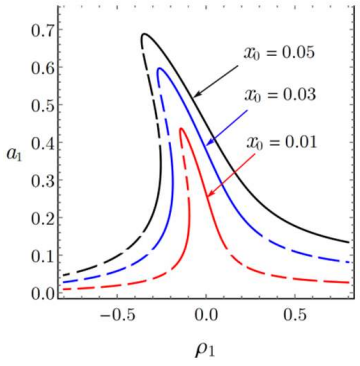

Fig. 4. FRC of the uncontrolled beam control under different values of amplitude of the support motion x_0

6.2 Nonlinear composite beam with positive position feedback (PPF) controller

The effectiveness of PPF controller on a forced and self-excited nonlinear beam is studied in this section. To minimize the beam response close to its natural frequency $\omega_1 = 3.06309$, we take PPF controller parameters such that its natural frequency $\omega_2 = \omega_1 + \sigma_2$ and $\sigma_2 = 0$. Other controller parameters are chosen properly.

Fig. 5 presents the time history and the Poincare map for the controlled beam under different values of self-excitation (α_1) at $x_0 = 0.01$, $\alpha_2 = 0.2$. It can be seen that system vibrates with a stable periodic motion. If self-excitation of the primary system increases to the extent that a quasi-periodic motion occurs, we can tune the controller damping coefficient α_2 to avoid this type of motion. However self-excitation α_1 in Fig. 5(b) is larger than that in Fig. 5(a), the system vibrations remain stable and periodic. If we compare Fig. 5 with Fig. 3, we can see that the PPF controller successes in elimination of effects of the self-excitation.

Fig. 6 presents a comparison between FRC of an uncontrolled beam and a controlled beam. We get a good vibration suppression bandwidth as indicated by the dashed rectangle in the figure. In addition, system is stable for a larger range of excitation frequency.

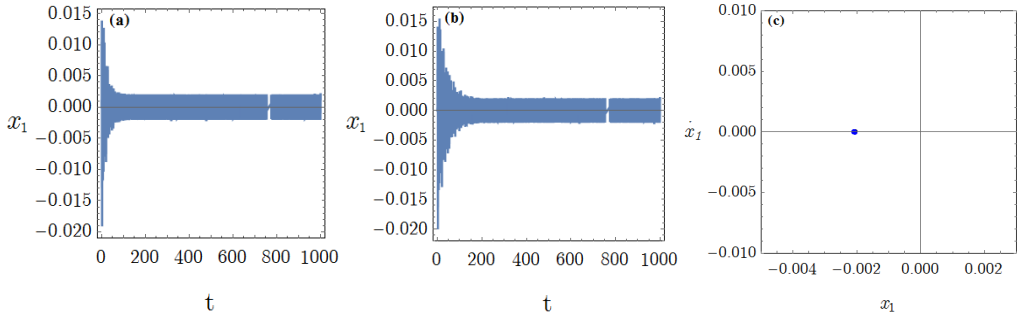

Fig. 5. (a) The time history of the controlled system at $\alpha_1 = 0.01$, (b) The time history of the controlled system at $\alpha_1 = 0.1$ and (c) Poincaré map, all at $x_0 = 0.01$, $\alpha_2 = 0.2$

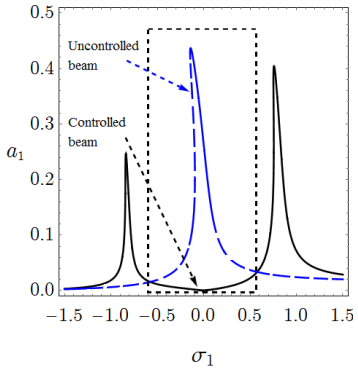

Fig. 6. Comparison between FRC of an uncontrolled beam and a controlled beam

Fig. 7 presents a numerical simulation of the FRC of the beam and controller, respectively by using numerical integration of original equations (5) and (6). The numerical results for steady sate solutions are plotted as small circles. If we compare Figs. 5 and 6 with Figs. 2 to 4, we can see a good vibration reduction and the effect of self-excitation is eliminated.

The effect of varying the amplitude of the support motion x_0 on the FRC of the beam and the controller is illustrated in Fig. 8. This figure shows that the minimum steady state displacement amplitude of the beam occurs at $\sigma_1 = 0$. So PPF controller successes in vibration suppression for a suitable bandwidth of excitation frequency Ω. When x_0 increases the peak displacement amplitudes increase also FRC bends away from the linear curves resulting in multivalued regions by jump phenomenon.

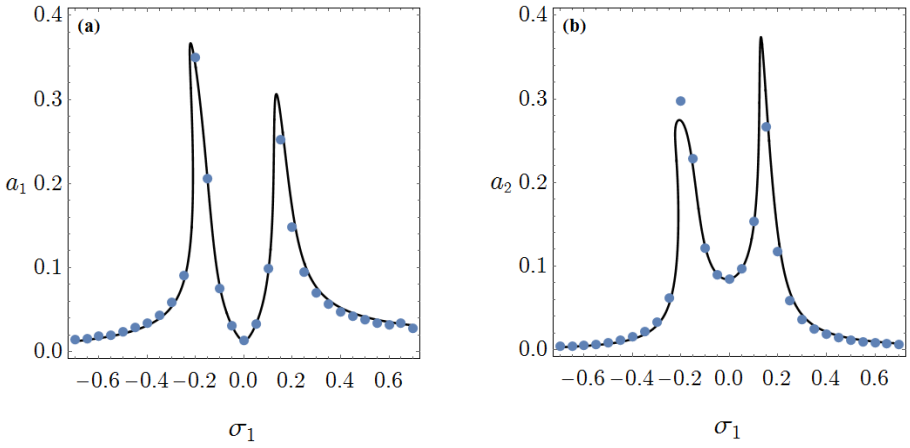

Fig. 7. Numerical simulation of FRC of (a) beam and (b) controller at $\alpha_2 = 0.05,\ \lambda_1 = \lambda_2 = 1$ and $x_0 = 0.01$.

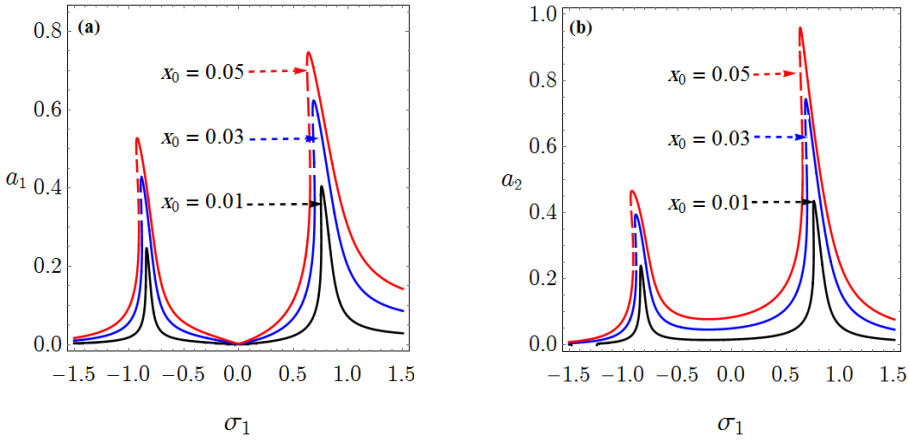

Fig. 8. FRC of (a) Beam and (b) Controller under different values of amplitude of the support motion x_0

Fig. 9 shows the effect of the controller's Linear damping coefficient α_2 on FRC of the beam and the controller, respectively. The figure shows that, for large values of α_2 both the beam and the controller exhibit linear responses in addition, the jumping phenomenon, multivalued solution regions and bifurcation points disappear. Also beam and controller peak displacement amplitudes decrease when α_2 increases which reduces the controller overload risk. So existence of multivalued solution region, jump phenomenon and bifurcation point depends on value of α_2 and α_2 is an important parameter in reducing controller's overload risk.

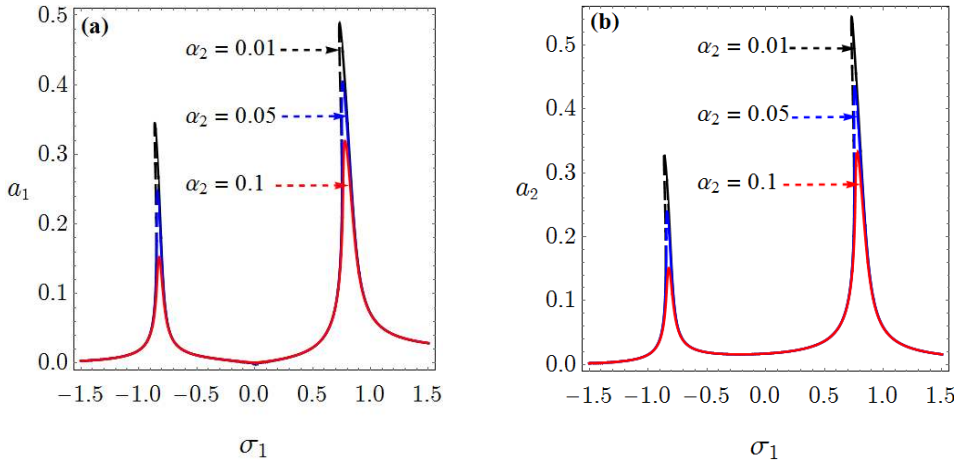

Fig. 9. FRC of (a) Beam and (b) Controller at different values of linear damping coefficient of the controller α_2

Fig. 10 presents the effects of the control signal gain λ_1 on FRC of the beam and the controller, respectively. Fig. 10(a) shows that vibration suppression bandwidth increases as control signal gain λ_1 increases. Also controller peak displacement amplitudes decrease as control signal gain λ_1 increases.

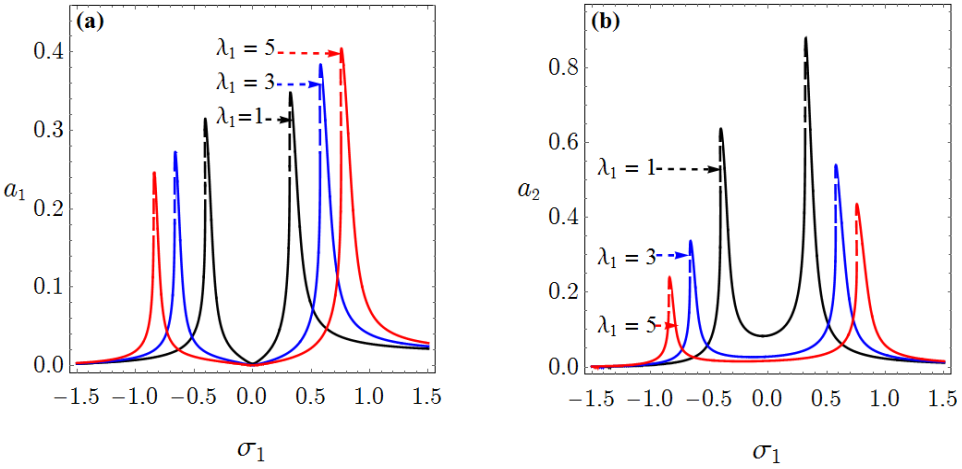

Fig. 10. FRC of (a) Beam and (b) Controller under different values of the control signal gain λ_1

The effects of positive control feedback gain λ_2 on FRC of beam and controller are shown in Fig. 11, respectively. In Fig. 11(a), it can be seen that vibration suppression bandwidth increases as feedback gain λ_2 increases so increasing λ_2 is good for vibration suppression process. Feedback gain λ_2 has similar effect to control signal gain λ_1 on FRC of beam. But Fig. 11(b) shows that, controller peak displacement amplitudes increase as feedback gain λ_2 increases which also increases the risk of controller overload. So it is better to widen the vibration suppression bandwidth by increasing λ_1.

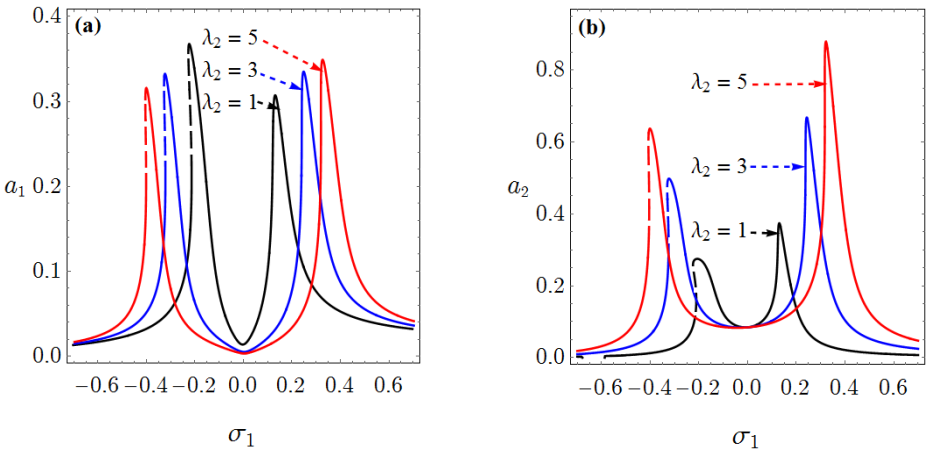

Fig. 11. FRC of (a) Beam and (b) Controller under different values of positive control feedback gain λ_2 at $\lambda_1 = 1$

In Figs. 6-12, it is clear that there is good vibration suppression around $\sigma_1 = 0$ however, for large values of $|\sigma_1|$ apart from 0 there are two peak displacement amplitudes of beam. To overcome this problem we can tune the controller natural frequency as studied in Fig. 12. The controller natural frequency can be tuned by changing the internal detuning parameter σ_2 depending on $\omega_2 = \omega_1 + \sigma_2$. Fig. 12(a) clears that minimum beam steady state displacement amplitude occurs when $\sigma_1 = \sigma_2$ i.e. ($\Omega = \omega_2$). From this result we can recommend to tune the controller natural frequency to be equal to excitation frequency for dynamical systems which are subjected to variable excitation frequency out illustrated vibration suppression bandwidth in Fig. 6.

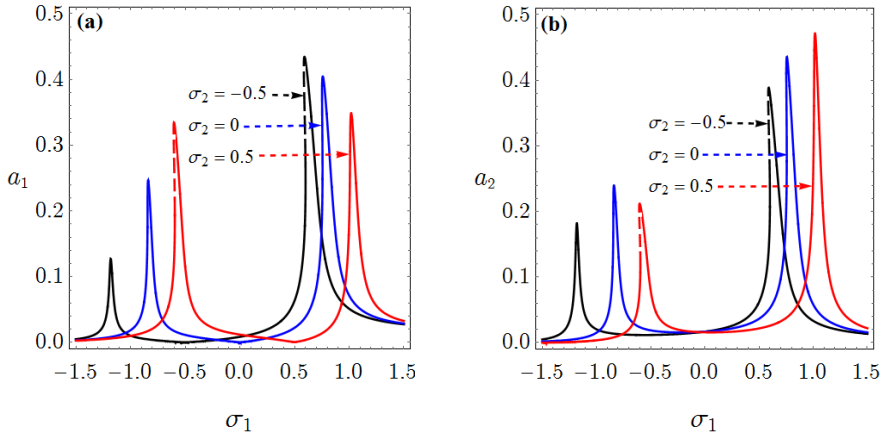

Fig. 12. FRC of (a) Beam and (b) Controller under different values of internal detuning parameter σ_2.

Force-amplitude response curve for the beam and the controller before and after control is presented in Fig. 13 under the condition $\sigma_1 = \sigma_2$ for controlled beam. Relation between beam displacement amplitudes and support motion displacement amplitude (excitation force amplitude) before using controller is a nonlinear relation which may produce large beam displacement amplitudes for a slight increase in support motion displacement amplitude and may contain jump phenomenon and unstable solution regions. After control under the condition $\sigma_1 = \sigma_2$, the relation became linear and the beam displacement amplitude

increases with extremely small values when support motion displacement amplitude increases. In addition, the controller displacement amplitude increases linearly with the support motion displacement amplitude. When condition $\sigma_1 = \sigma_2$ isn't satisfied such that difference between σ_1 and σ_2 isn't small and we found that controller efficiency in vibration suppression decreases but the controlled beam displacement amplitudes still smaller than that of uncontrolled beam. Fig. 14 verifies the result in Fig. 13 at $\sigma_1 = \sigma_2 = 0$.

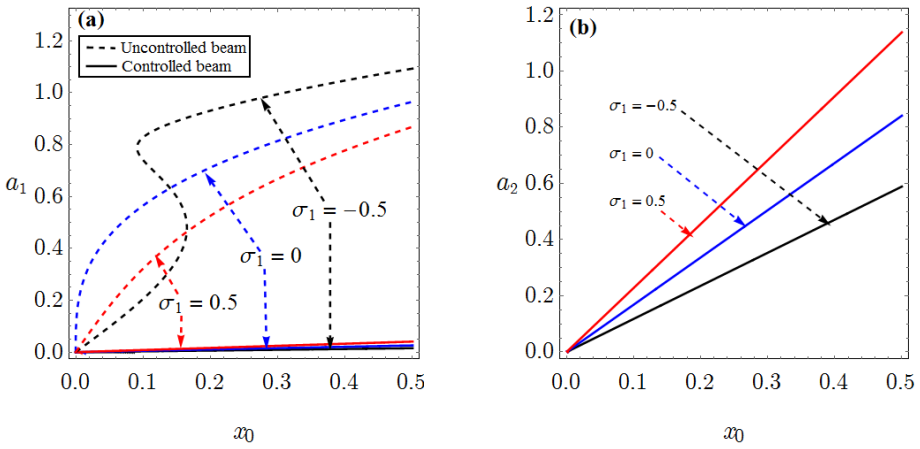

Fig. 13. Force-amplitude response curve of (a) Beam and (b) Controller at different values of σ_1 under the condition $\sigma_1 = \sigma_2$ in case of controlled beam

The effect of varying controller natural frequency ω_2 on FRC of the beam and the controller is studied in Fig. 15 at different values of σ_1. We vary controller natural frequency ω_2 by varying value of internal detuning parameter σ_2 as $\omega_2 = \omega_1 + \sigma_2$. The minimum steady-state displacement amplitude of the beam occurs at $\sigma_2 = \sigma_1$ which insures result of Fig. 13. This is the optimal case for controller operation ($\sigma_2 = \sigma_1$). When value of σ_2 tends more to value of σ_1, vibration suppression is better as shown in the targeted region in the figure. The figure also illustrates that, in case of mistuning ($\sigma_2 \neq \sigma_1$), it is preferred to adjust ω_2 I.e. $\sigma_2 \leq \sigma_1$ or ($\omega_2 \leq \Omega$) to be sure that the system is stable.

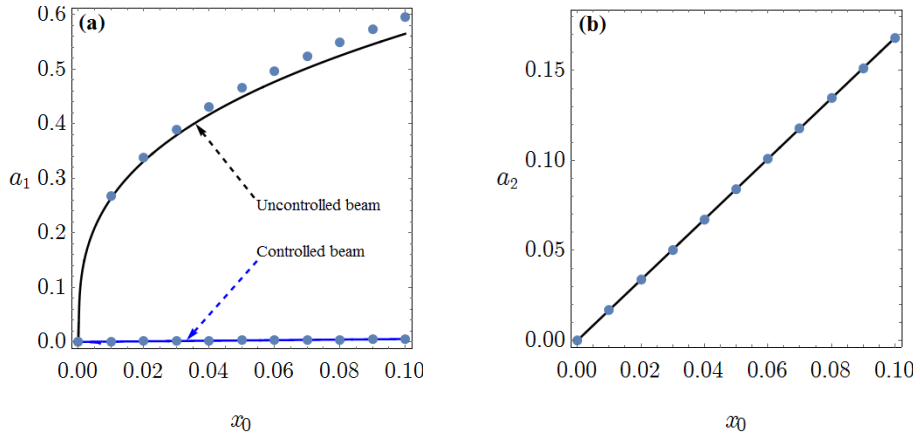

Fig. 14. Numerical simulation of force- amplitude response curve of (a) Beam and (b) Controller at $\sigma_1 = \sigma_2 = 0$

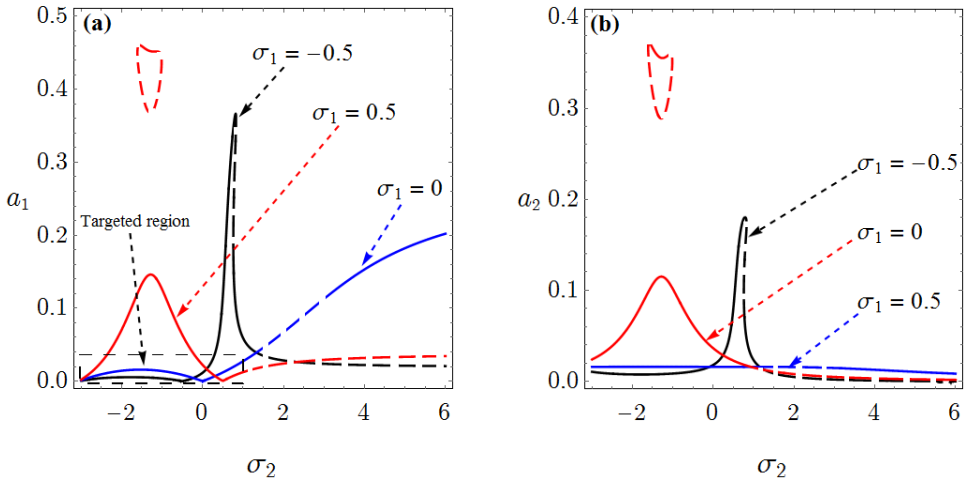

Fig. 15. Effect of varying controller natural frequency on FRC of (a) Beam and (b) Controller at different values of σ_1

7 Conclusion

In this paper, positive position feedback PPF controller is applied to a nonlinear beam with self and external excitations in primary resonance case and presence of 1:1 internal resonance. Analytical and numerical results which have been obtained show that: there is a good vibration suppression bandwidth especially at $-0.5 \le \sigma_1 \le 0.5$, see Fig. 3. There is a good vibration suppression in spite of increasing of support motion amplitude x_0, see Fig. 4. When linear damping coefficient of controller α_2 increase, the peak displacement amplitudes of the beam and controller decrease and controller overload risk decreases. Vibration suppression bandwidth can be increased by increasing controller or/and feedback gains. So it is better to widen the vibration suppression bandwidth by increasing λ_1 as increasing λ_2 increases the controller overload risk. PPF controller successes in elimination of self-excitation effects, see Fig. 5.

For large values of $|\sigma_1|$ apart from 0 there are two peak displacement amplitudes of beam. This problem can be solved by tuning the controller natural frequency such that $\Omega = \omega_2$ where the minimum beam steady state displacement amplitude occurs at $\sigma_2 = \sigma_1$, see Fig. 12. From this result we can recommend to tune the controller natural frequency to be equal to excitation frequency for dynamical systems which are subjected to variable excitation frequency out the original vibration suppression bandwidth around $\sigma_1 = 0$. This tuning process can be applied practically if the rate of change of excitation frequency can be accompanied by tuning controller natural frequency i.e. $\Omega = \omega_2$.

If PPF controller is properly tuned, the vibration suppression process is well and peak displacement amplitudes won't occur practically. In case of mistuning ($\sigma_2 \neq \sigma_1$), it is preferred to adjust ω_2 i.e. $\sigma_2 \le \sigma_1$ or ($\omega_2 \le \Omega$) to be sure that the system is stable, see Fig. 15.

Competing Interests

Authors have declared that no competing interests exist.

References

[1] Abadi. Nonlinear dynamics of self-excitation in auto parametric systems. University of Utrecht, Netherlands; 2003.

[2] El-Badawy AA, Nasr El-Deen TN. Quadratic nonlinear control of a self-excited oscillator. Journal of Vibration and Control. 2007;13(4):403–414.

[3] Jun L, Xiaobin L, Hongxing H. Active nonlinear saturation-based control for suppressing the free vibration of a self-excited plant. Communications in Nonlinear Science and Numerical Simulation. 2010;15(4):1071–1079.

[4] Ouakad HM, Nayfeh AH, Choura S, Najar F. Nonlinear feedback controller of a microbeam resonator. Journal of Vibration and Control. 2015;21(9):1680–1697.

[5] Golnaraghi MF. Regulation of flexible structures via nonlinear coupling. Dynamics and Control. 1991;1:405–428.

[6] Duquette AP, Tuer KL, Golnaraghi MF. Vibration control of a flexible beam using a rotation internal resonance controller part 1 theoretical development and analysis. Journal of Sound and Vibration. 1993;167(1):41–62.

[7] Duquette AP, Tuer KL, Golnaraghi MF. Vibration control of a flexible beam using a rotation internal resonance controller part 2 experiment. Journal of Sound and Vibration.1993;167(1):63–75.

[8] Jun L, Hongxing H, Rongying S. Saturation-based active absorber for a non-linear plant to a principal external excitation. Mechanical Systems and Signal Processing. 2007;21(3):1489–1498.

[9] Pai PF, Wen B, Naser AS, Schulz MJ. Structural vibration control using PZT patches and non-linear phenomena. Journal of Sound and Vibration. 1998;215(2):273–296.

[10] Tondl A, Nabergoj R, Ecker H. Quenching of self-excited vibrations in a system with two unstable vibration modes. Vibration Problems ICOVP. 2005;487–492.

[11] Tondl A, Nabergoj R. The effect of parametric excitation on a self-excited three-mass system. International Journal of Non-Linear Mechanics. 2004;39(5):821–832.

[12] Pust L, Tondl A. System with a non-linear negative self-excitation. International Journal of Non-Linear Mechanics. 2008;43(6):497–503.

[13] Verhurlst F. Quenchening of self-excited vibrations. Journal of Engineering Mathematics. 2005;53: 349–358.

[14] Szabelski K, Warminski J. Vibrations of a non-linear self-excited system with two degrees of freedom under external and parametric excitation. International Journal of Nonlinear Dynamics. 1997;14:23–36.

[15] Szabelski K, Warminski J. The self-excited system vibrations with the parametric and external excitations. Journal of Sound and Vibration. 1995;187(4):595–607.

[16] Szabelski K, Warminski J. The parametric self-excited non-linear system vibrations analysis with the inertial excitation. International Journal of Non-Linear Mechanics. 1995;30(2):179–189.

[17] Warminski J. Regular and chaotic vibrations of a parametrically and self-excited system under internal resonance condition. Meccanica. 2005;40:181–202.

[18] Warminski J. Synchronization effects and chaos in van der pol-mathieu oscillator. Journal of Theoretical and Applied Mechanics. 2001;4(39):861–884.

[19] Warminski J, Cartmell MP, Mitura A, Bochenski M. Active vibration control of a nonlinear beam with self- and external excitations. Shock and Vibration. 2013;20:1033–1047.

[20] Jian Xu, Chen Y, Chung KW. An improved time-delay saturation controller for suppression of nonlinear beam vibration. Nonlinear Dyn. 2015;82:1691–1707.

[21] Nayfeh AH, Mook DT. Nonlinear oscillations. New York: Wiley; 1979.

Appendix

$$r_{11}=\frac{\alpha_1}{2}-\frac{9}{8}a_{10}^2\beta_1\omega_1^2,\ r_{12}=\frac{\mu\,\Omega^2\sin(\varphi_{10})\,x_0}{2\omega_1},\ r_{13}=\frac{\sin(\varphi_{20})\,\lambda_1}{2\omega_1},\ r_{14}=\frac{\cos(\varphi_{20})\,a_{20}\,\lambda_1}{2\omega_1},$$

$$r_{21}=\frac{1}{8\,a_{10}^2\,\omega_1}\Big(-4\,\mu\,\Omega^2\sin(\varphi_{10})\,x_0-6\,a_{10}^3\gamma_1-4\cos(\varphi_{20})\,a_{20}\,\lambda_1+4\,\delta\,a_{10}^3\,\omega_1^2\Big),\ r_{22}=\frac{\mu\,\Omega^2\cos(\varphi_{10})\,x_0}{2\,a_{10}\,\omega_1},$$

$$r_{23}=\frac{\cos(\varphi_{20})\lambda_1}{2a_{10}\omega_1},\ r_{24}=-\frac{\sin(\varphi_{20})a_{20}\lambda_1}{2a_{10}\omega_1},\ r_{31}=-\frac{\sin(\varphi_{20})\lambda_2}{2\omega_2},\ r_{32}=0,\ r_{33}=-\frac{\alpha_2}{2},\ r_{34}=-\frac{\cos(\varphi_{20})a_{10}\lambda_2}{2\omega_2},$$

$$r_{41}=\frac{-2\cos(\varphi_{20})\,a_{10}^2\,\lambda_2\,\omega_1-2\,a_{20}\Big(\mu\,\Omega^2\sin(\varphi_{10})\,x_0+\cos(\varphi_{20})\,a_{20}\,\lambda_1\Big)\omega_2+a_{10}^3\,a_{20}\Big(-3\,\gamma_1+2\,\delta\,\omega_1^2\Big)\omega_2}{4\,a_{10}^2\,a_{20}\,\omega_1\,\omega_2},$$

$$r_{42}=\frac{\mu\,\Omega^2\cos(\varphi_{10})\,x_0}{2\,a_{10}\,\omega_1},\ r_{43}=\frac{3\,a_{10}\,a_{20}^3\,\gamma_2\,\omega_1+2\cos(\varphi_{20})\,a_{10}^2\,\lambda_2\,\omega_1+2\,a_{20}^2\,\lambda_1\cos(\varphi_{20})\,\omega_2}{4\,a_{10}\,a_{20}^2\,\omega_1\,\omega_2},$$

$$r_{44}=\frac{4\sin(\varphi_{20})\,a_{10}^2\,\lambda_2\,\omega_1-4\sin(\varphi_{20})\,a_{20}^2\,\lambda_1\,\omega_2}{8\,a_{10}\,a_{20}\,\omega_1\,\omega_2}.$$

Peer-review history:
The peer review history for this paper can be accessed here (Please copy paste the total link in your browser address bar)
http://sciencedomain.org/review-history/15199